Published as: Smart Mater. Struct. 29 (2020) 117002 https://doi.org/10.1088/1361-665X/abadd3

A piezoelectric self-powered active interface for AC/DC power conversion improvement of electromagnetic energy harvesting

G Lombardi[1], M Lallart[1], M Kiziroglou[2] and E M Yeatman[2]

[1]Univ. Lyon, INSA Lyon, LGEF, EA682, F 6 9621, VILLEURBANNE, FRANCE
[2]Department of Electrical and Electronic Engineering, Imperial College London, Exhibition Road, London, SW7 2AZ, United Kingdom

E-mail: mickael.lallart@insa-lyon.fr

Abstract. In the framework of hybrid energy harvesting for scavenging ambient motion, this paper proposes a cooperative piezoelectric electromagnetic energy harvesting system to harvest rotational energy. In particular, while the actual process of harvesting energy is accomplished by the electromagnetic device, the piezoelectric element is used for improving the AC/DC conversion efficiency of the former. To do so, a half wave voltage doubler using MOSFETs driven by a piezo element is employed. The low voltage output (order of magnitude of mV) of the electromagnetic system and the low conversion abilities of the piezoelectric transducer in the proposed mechanical structure justifies the motivation behind this work. Simulations followed by the experimental validations are exposed and discussed, highlighting the improvement of energy conversion efficiency of an electromagnetic transducer, giving a power gain of 27 with respect to the DC power obtained with standard silicon diodes.

Keywords: energy harvesting, hybrid system, AC/DC power conversion efficiency, electromagnetic systems, piezoelectric systems

1. Introduction

With the spread of the "Internet of Things" (IoT), expectations arise regarding a wide infrastructure network of low-powered devices that will allow to collect and exchange data in an autonomous and independent way. To collect informations, sensors with different functionalities can be installed, such as detecting temperature variations, humidity, strain distributions, etc. [1]. However, the main concern is the durability and independence to energy source of these sensing nodes when they are installed in hostile or confined/remote locations, as they are normally powered by batteries, which have limited lifetime and require regular replacement [2]. A promising alternative to batteries is the concept of harnessing waste energy from the environment (such as vibration, light, temperature gradients) to power these sensor nodes [3, 4]. Among

the available energy sources, rotational motion provides widespread devices: it is in fact the most common way to produce electricity for large-scale power generation devices. In order to efficiently extract this form of energy at a small scale in a readily available manner, the most straightforward solution is to miniaturize conventional electromagnetic generators (EMG), leading to the development of micro-rotational electromagnetic energy harvesters, extensively developed in the last decade and being able to reach the typical power levels required to power sensors (few hundreds of μW or more) [5–9].

In addition to electromagnetic (EM) conversion, piezoelectric (PZT) conversion has also been widely adopted in rotational energy harvesting, using various concepts according to the principle of excitation [10, 11]. A typical one consists of a piezoelectric cantilever beam fixed on a stationary base with its tip magnet interacting with a moving magnet mounted on a rotating host. Due to magnetic plucking, the phenomenon of frequency up-conversion is then observed [12–15]. However, these systems are often characterized by lower energy density with respect to rotational electromagnetic systems. Nevertheless, despite the relatively high power levels that can be extracted from electromagnetic energy harvesters in a rotational environment, these are most often distinguished by low output voltage (order of magnitude of mV). For this reason, EMG suffer from low AC/DC power conversion efficiency, as most of the potential energy that can be extracted is lost in the rectification circuit of the power management unit.

A possible improvement of the rectification efficiency can be achieved involving active rectifiers. This can be realized by controlling MOSFETs using active circuits (e.g., Op-Amps). In this way, the typical voltage drops occurring across standard diodes are largely avoided. However, these active components have the requirement to be powered with a minimum operating voltage (at least few hundreds of milliVolts [16]) and constantly draining power from the system. Also, the issue of cold-starting (*i.e.* when no energy is present in a local electrical component) is a particular challenge to tackle. Turning these active elements on from a complete unpowered state can thus be highly complex (for instance, involving further specific functionalities in the circuit [17–19]) and potentially time and energy consuming, as it is necessary to power these systems before the main circuit (thus, actually delaying the harvesting process from the electromechanical system).

In recent years, researchers have started to combine multiple energy conversion mechanisms in the same structure, exploiting different or the same energy source by the use of more than one transducer, making the system hybrid [20–26]. Nonetheless, one issue when dealing with hybrid systems is the difference in terms of voltage and power levels that the transducers exhibit, which adds complexity to the harvesting process on the circuit side. Another option, which addresses this deficiency, is to use the secondary, and often weaker, power source as an auxiliary biasing voltage source for power management circuitry. In this direction, examples using solar [27], thermal [28, 29] or kinetic [30] sources to bias far-field radio frequency (RF) harvesters have been proposed.

Exploiting available energies from different sources at very different frequency levels might not be accessible in all kinds of environment. A valid yet seldom alternative to the previously mentioned techniques, is to use electromechanical systems exploiting mechanical vibrations as the sole energy source. Hence, in this work, a hybrid cooperative electromagnetic-piezoelectric energy harvester extracting vibrational energy is proposed. The work focuses on the power conversion efficiency improvement of the electromagnetic transducer employing MOSFETs that are powered by the piezoelectric system. The paper is organized as follows: Section 2 illustrates the motivation behind the proposed work and the operating principles of the presented scheme; Section 3 aims at experimentally validating the hybrid cooperative system; finally, Section 4 briefly concludes the paper.

2. Motivation and operating principles

This section aims at discussing the main motivation and principles of the proposed active self-powered interface. The hybrid electromagnetic-piezoelectric energy harvesting system has been derived from the rotational system previously developed by H. Fu *et. al* [12]. It consists of a piezoelectric beam installed below a rotating host, with a tip magnet placed at its free end. As the rotating platform contains a cuboidal magnet as well, the magnetic force exerted between the driving magnet and the tip magnet plucks the piezoelectric beam periodically, making it to vibrate at its resonance frequency in a frequency-up conversion manner. Previous works have demonstrated to be able to harvest up to 10-20 μW, which is typically less than what can be potentially harvested from electromagnetic systems exploiting the same energy source. Hence, in order to further exploit the energy that is already available in the system, a coil is placed above the rotating host: a voltage is thus induced across the coil due to the variation of the magnetic flux generated by the moving magnet. Figure 1 thus depicts the experimental measurements of the AC output powers (obtained by connecting the transducer to a parallel resistor R_L) from the piezoelectric and the electromagnetic systems. The maximal AC power from the electromagnetic system corresponds to 208 μW, one order of magnitude of difference with respect to the piezoelectric AC power output (10 μW).

These results demonstrate the limitations, in the considered structure, of the piezoelectric transducer for directly extracting energy from rotational systems compared to the electromagnetic ones. However, despite having relatively high power levels that can potentially be extracted from the electromagnetic system, the electromagnetic voltage output levels are anyway lower than the typical diode threshold voltage (0.6 V). This would eventually lead to high power losses when rectifying the AC voltage to a DC stage (as sensors need to be powered in continuous current). Meanwhile, in spite of the significantly lower power output, the piezoelectric element shows voltage of several volts. A comparison between the experimental open-circuit voltage of the piezoelectric and electromagnetic systems is shown in figure 2 ‡.

‡ The measurements of such waveforms were not conducted at the same time as the purpose was to

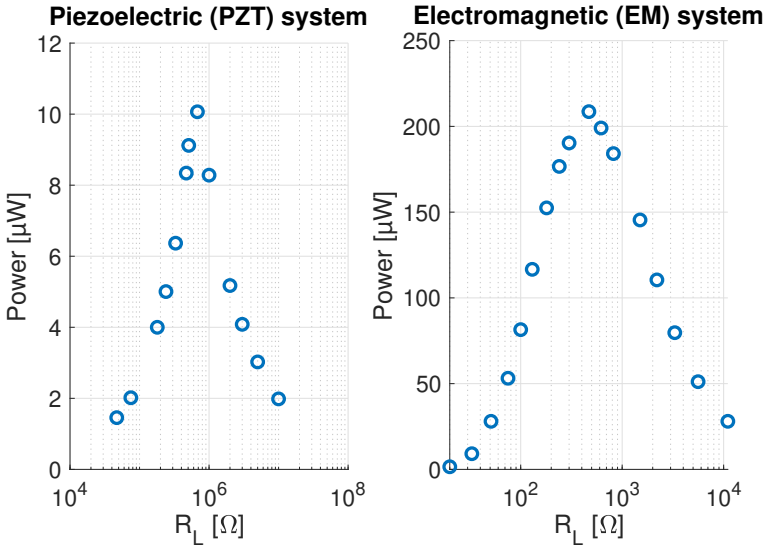

Figure 1: Experimental AC powers for the piezoelectric and electromagnetic systems

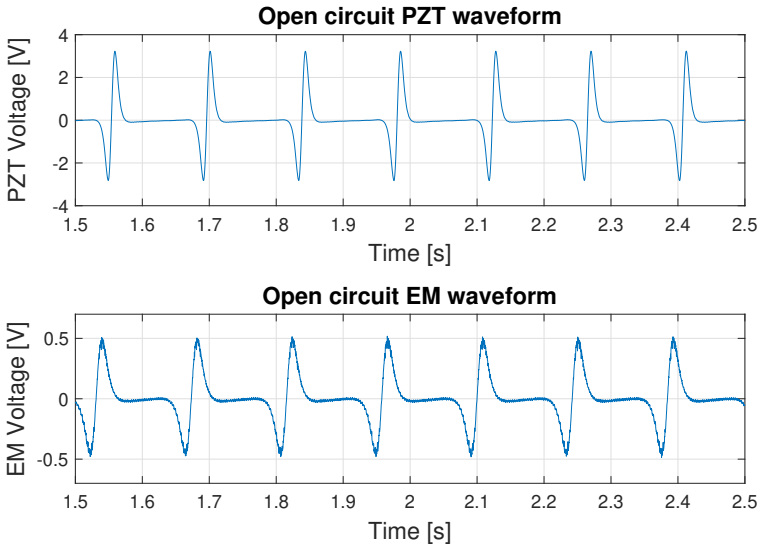

Figure 2: Experimental open-circuit voltage waveforms for the piezoelectric and the electromagnetic systems

To overcome the EMG low AC/DC power conversion efficiency drawback while taking advantage of the voltage levels of the piezoelectric transducer, the idea behind the proposed hybrid interface is to replace the standard diodes normally used for rectification by MOSFETs that are directly powered by the piezoelectric system. The resulting circuit is illustrated in figure 3, consisting of a half-wave voltage doubler composed of two capacitors C_1 and C_2 and two MOSFETs (p-MOS and n-MOS transistors, for the negative half-wave and the positive half-wave, respectively), which replace the diodes. The gate voltage (V_G) of the used transistors is provided by the piezoelectric transducer

conduct an initial investigation of the voltage waveforms and related powers

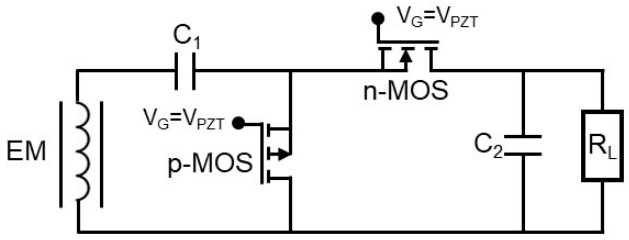

Figure 3: Circuit schematic

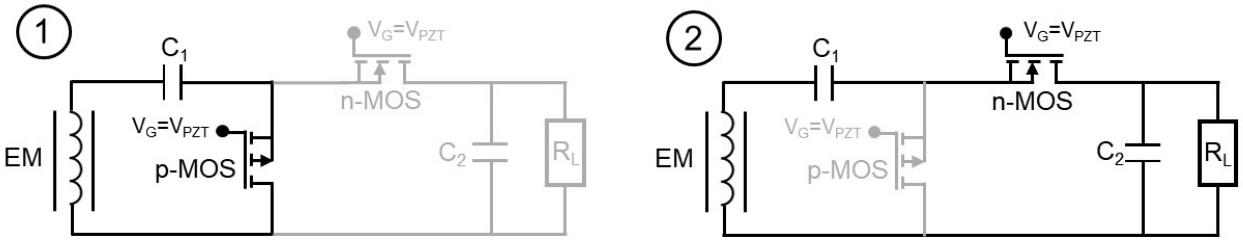

(a) Negative half-cycle (b) Positive half-cycle

Figure 4: Circuit operations

(V_{PZT}), controlling the ON and OFF states of the MOSFETs. The principles is to charge the C_1 and C_2 capacitors with the peak values of the input electromagnetic source by properly synchronizing the activation and deactivation of the MOSFETs.

In particular, the main operating phases of the circuit are the followings:

- Negative half-cycle: during the negative half-cycle the p-MOS gets activated by the negative piezoelectric voltage, acting like a forward biased diode, as in figure 4a. This allows the charge of the capacitor C_1 until the voltage across it becomes

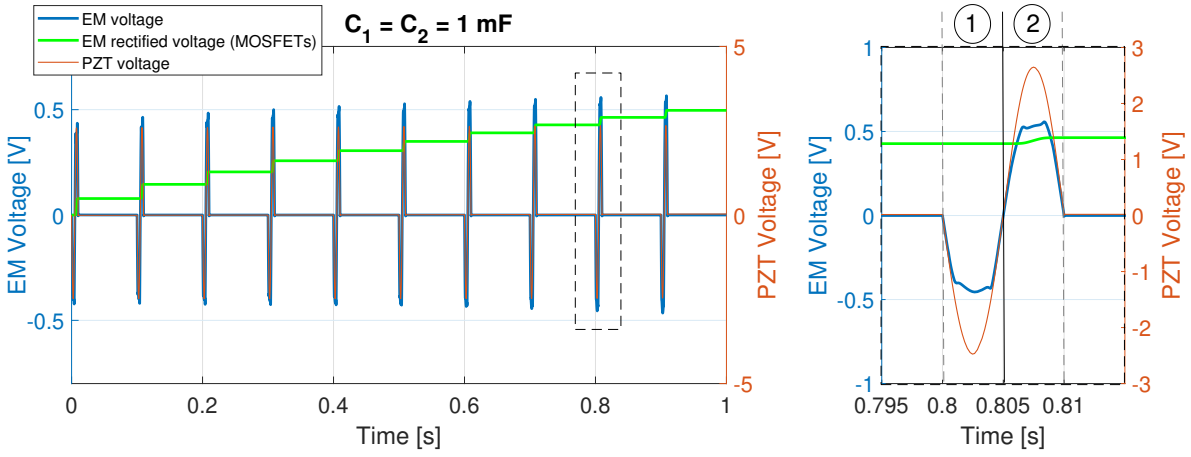

Figure 5: Simulated voltage waveforms (the value of capacitance has been chosen in order to enhance the charge of the capacitors for each cycle); ①: Negative half-cycle; ②: Positive half-cycle

equal to the AC electromagnetic voltage peak. During this phase the n-MOS is deactivated so that the electromagnetic system is not connected to the capacitor C_2 and the load R_L. This state corresponds to the phase ① depicted in figure 5;

- Positive half-cycle: during the positive half-cycle the n-MOS gets activated by the positive piezoelectric voltage while having the p-MOS deactivated, as shown in figure 4b. The capacitor C_2 is then charged until the voltage across it becomes equal to the sum of the AC electromagnetic voltage peak and the voltage across C_1 (previously charged during the negative half-cycle). This state corresponds to phase ② depicted in figure 5;
- As the electromagnetic system returns to the negative half-cycle, the n-MOS is turned off again and the process repeats.

It has to be noted that the capacitor C_2 discharges through the load R_L during all the stages involved (even when receiving the extra charges after phase 2).

The above considerations evidence the importance of the proper synchronization of the piezoelectric and electromagnetic voltage peaks (negative and positive - as shown in figure 5), which have to occur at the same time in order to properly activate the MOSFETs. As a preliminary validation process, LTSpice simulations have been conducted. Figure 5 shows the simulated waveforms of the electromagnetic and piezoelectric voltages and the rectified electromagnetic (EM) voltage obtained through the proposed hybrid approach. The value of capacitances involved has been chosen to be equal to $1mF$ (for both C_1 and C_2) in order to highlight the charging process of the capacitors during each cycle. The magnified waveform on the right of figure 5 illustrates in a more visible way both the electromagnetic and piezoelectric voltage peaks (occurring at the same instant) and the resulting rectified EM voltage.

Figure 6 depicts the simulated waveforms in the transient state. In order to demonstrate the benefits of the proposed hybrid rectification, the cases of using Schottky diodes and standard silicon diodes have been considered as well. This figure clearly demonstrates the enhancement of the rectified electromagnetic voltage with respect to the Schottky diodes rectification and, more particularly, to the standard diodes rectification.

With the aim of illustrating the influence of the piezoelectric voltage on the activations of the MOSFETs and the final AC/DC conversion efficiency, simulations using various input piezoelectric and electromagnetic voltage magnitudes were conducted. Figure 7a illustrates the schematic of the simulation: for the sake of simplicity, both the piezoelectric and electromagnetic sources are represented by pulsed sine wave signals. The piezoelectric system (modelled as a voltage source in series with a capacitor) is connected to the gate of the MOSFETs (ZVP4424A for the p-MOS and ZVNL120A for the n-MOS), controlling their ON and OFF states. The electromagnetic transducer (modelled as a voltage source in series with a resistor §) is directly connected to the half-wave voltage doubler employing the piezoelectric-powered MOSFETs.

§ The inductance is negligible for the considered frequency

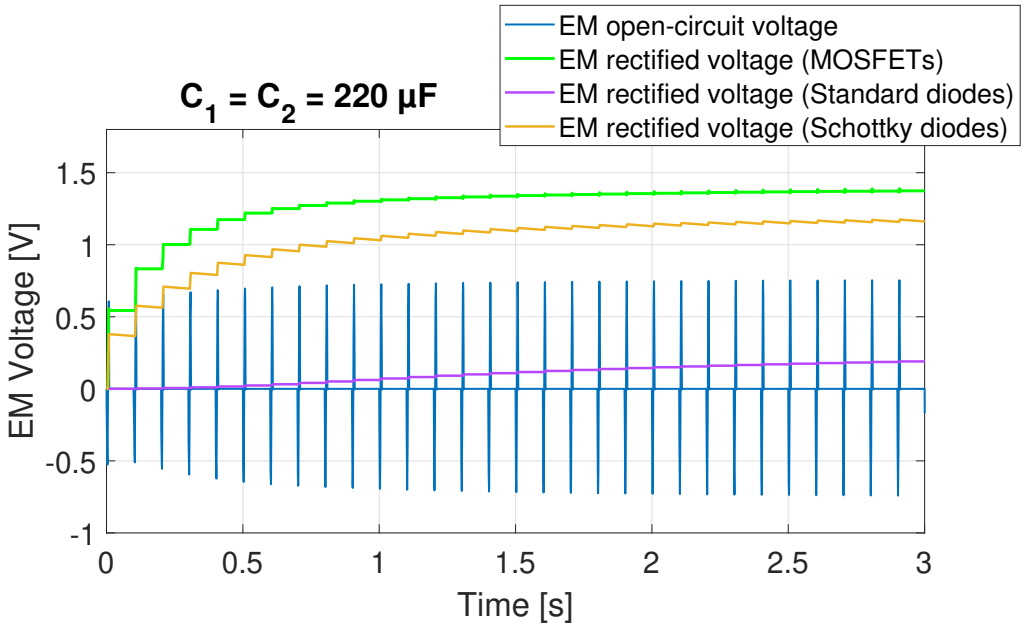

Figure 6: Simulated transient waveforms

For each case, the DC powers obtained with the cooperative hybrid method were evaluated and compared with the cases of using Schottky diodes (figure 7b) and standard silicon diodes (figure 7c), as shown in the schematic. Table 1 compares the maximum output powers P_{max} and the related conversion ratio η between the DC output power $P_{EM,DC}$ and the AC electromagnetic $P_{EM,AC}$ and piezoelectric $P_{PZT,AC}$ powers of the analysed techniques, as defined as:

$$\eta = \frac{P_{EM,DC}}{P_{EM,AC} + P_{PZT,AC}} \times 100\% \tag{1}$$

For fair comparison, the piezoelectric power $P_{PZT,AC}$ has been considered in the calculation of η in the hybrid case only. It has to be noted that such a conversion efficiency has the aim of highlighting the AC/DC conversion improvement from a purely electrical point of view. The energy conversion efficiency of the involved traducers due to the harvesting process is thus not taken into account.

The results shown in the table evidence the influence of the piezoelectric voltage in the final harvested power and its related conversion efficiency for the hybrid case. In fact, increasing the piezoelectric output voltage leads to an increment of the power that can be harvested with the electromagnetic system. However, the input piezoelectric energy to be taken into account on the of the conversion efficiency increases as well, thus leading to an optimal value of piezoelectric input voltage of 4.5 V for the both considered cases of electromagnetic open-circuit voltages. This is further clarified in figure 8, plotting the obtained conversion efficiencies as a function of the input piezoelectric voltage.

Finally, an equivalent maximum DC power when considering an ideal behaviour of the diodes $P_{DC,ideal}$ (without taking into account the diodes losses) can be derived

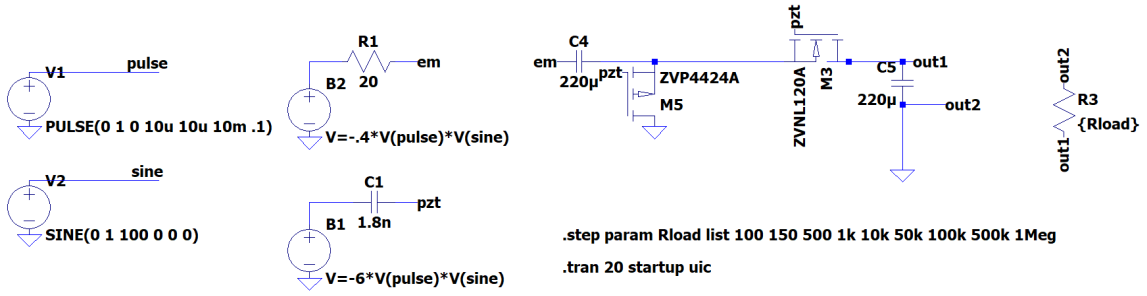

(a) Simulation of the hybrid cooperative electromagnetic-piezoelectric interface

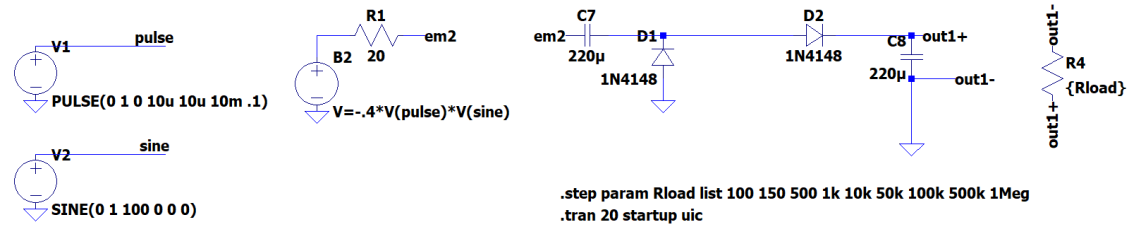

(b) Simulation of the half-wave voltage doubler interface employing Schottky diodes

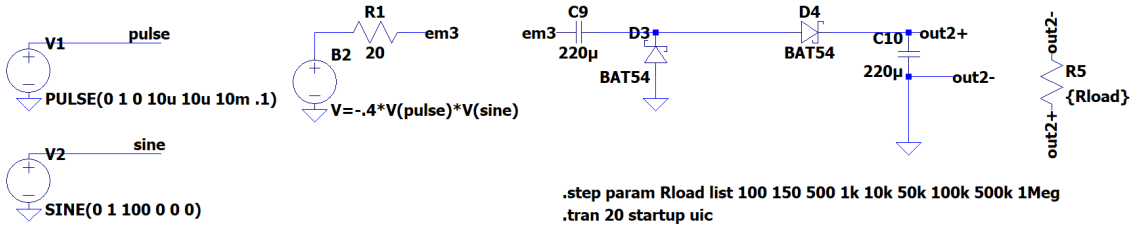

(c) Simulation of the half-wave voltage doubler interface employing Standard silicon diodes

Figure 7: Schematic of the LTSice simulations

Table 1: Comparison of simulated maximum powers and related conversion efficiencies

	Case 1: $V_{EM,oc} = 0.7V$		Case 2: $V_{EM,oc} = 0.4V$	
	$P_{EM,AC} = 215\mu W$		$P_{EM,AC} = 60\mu W$	
	P_{max}	η	P_{max}	η
Standard diodes	3 μW	1.3 %	0.015 μW	0.025 %
Schottky diodes	72 μW	33 %	8 μW	13 %
Hybird ($V_{PZT_{peak}} = 1.5V$)	18 μW	9 %	10 μW	12 %
Hybird ($V_{PZT_{peak}} = 2V$)	73 μW	34 %	17 μW	28 %
Hybird ($V_{PZT_{peak}} = 3V$)	122 μW	56 %	38 μW	58 %
Hybird ($V_{PZT_{peak}} = 4.5V$)	170 μW	75 %	50 μW	70 %
Hybird ($V_{PZT_{peak}} = 6V$)	174 μW	72 %	52 μW	65 %

assuming that in steady-state conditions the capacitor C_1 is charged to a value equivalent

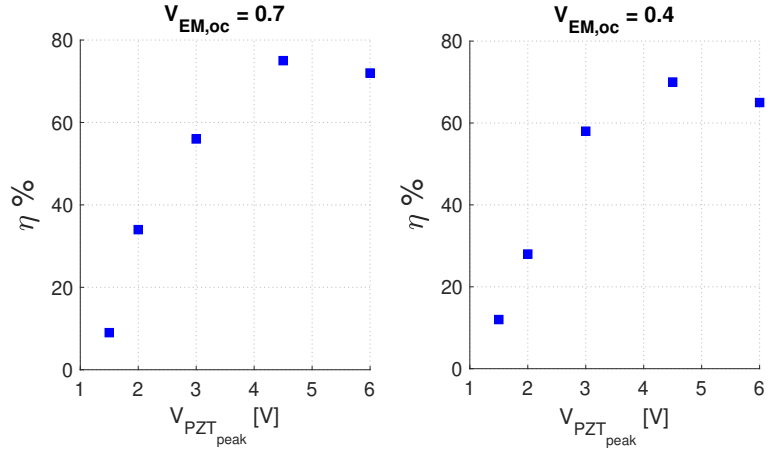

Figure 8: Conversion efficiencies for the hybrid piezoelectric-electromagnetic harvesting interface versus the piezoelectric voltage

to $\frac{V_{EM,DC}}{2}$ (being $V_{EM,DC}$ the DC voltage of the electromagnetic system) and considering that the conduction event during the positive half-cycle occurs when the following condition is reached:

$$V_{EM,oc}\sin(\omega t) + \frac{V_{EM,DC}}{2} > V_{EM,DC} \tag{2}$$

where the electromagnetic source is modelled as a sinusoidal voltage source of angular frequency ω. The conduction instant can be thus defined as:

$$t_1 = \frac{1}{\omega}\arcsin\left(\frac{1}{2}\frac{V_{EM,DC}}{V_{EM,oc}}\right) \tag{3}$$

thus giving the harvested energy for one conduction event:

$$\begin{aligned} E &= \int_{t_1}^{\frac{\pi}{\omega}-t_1} V_{EM,DC} I dt \\ &= \frac{V_{EM,DC}}{2r_c\omega}\left[4V_{EM,oc}\sqrt{1-\left(\frac{1}{2}\frac{V_{EM,DC}}{V_{EM,oc}}\right)^2} + V_{EM,DC}\left(2\arcsin\left(\frac{1}{2}\frac{V_{EM,DC}}{V_{EM,oc}}\right)-\pi\right)\right] \end{aligned} \tag{4}$$

where r_c is the coil resistance. The related ideal power $P_{DC,ideal}$ is obtained considering one harvesting event per period:

$$P_{DC,ideal} = \left[4V_{EM,oc}\sqrt{1-\left(\frac{1}{2}\frac{V_{EM,DC}}{V_{EM,oc}}\right)^2} + V_{EM,DC}\left(2\arcsin\left(\frac{1}{2}\frac{V_{EM,DC}}{V_{EM,oc}}\right)-\pi\right)\right] \times \frac{V_{EM,DC}}{4\pi r_c} \tag{5}$$

Table 2: Comparison of conversion efficiencies η_{DC} for different techniques

	Case 1: $V_{EM,oc} = 0.7V$	Case 2: $V_{EM,oc} = 0.4V$
	$P_{DC,ideal} = 162\mu W$	$P_{DC,ideal} = 45\mu W$
	η_{DC}	η_{DC}
Standard diodes	1.8 %	0.03 %
Schottky diodes	44 %	17 %
Hybird ($V_{PZT_{peak}} = 1.5V$)	11 %	21 %
Hybird ($V_{PZT_{peak}} = 2V$)	45 %	36 %
Hybird ($V_{PZT_{peak}} = 3V$)	73 %	76 %
Hybird ($V_{PZT_{peak}} = 4.5V$)	97 %	89 %
Hybird ($V_{PZT_{peak}} = 6V$)	94 %	80 %

When comparing the DC ideal powers (obtained with the voltage doubler interface employing ideal diodes) with the original AC power of the electromagnetic system, $P_{DC,ideal}$ actually reaches 75% of the power that can be measured when simply connecting the electromagnetic system to a resistor. Hence, an equivalent conversion efficiency η_{DC} with respect to the DC power limit when considering ideal diodes is also given for comparison purposes:

$$\eta_{DC} = \frac{P_{EM,DC}}{P_{DC,ideal} + P_{PZT,AC}} \times 100\% \tag{6}$$

Table 2 compares the conversion efficiencies η_{DC} of the different techniques when considering the same condition of voltage magnitudes of table 1. Once again, for the hybrid technique, the optimal piezoelectric voltage is achieved for $4.5V$ allowing reaching a theoretical conversion efficiency of 97%.

3. Experimental validation

3.1. Experimental set-up

In order to experimentally validate the theoretical predictions of the proposed hybrid cooperative active rectification, the set-up illustrated in figure 9 was implemented. It consists of a piezoelectric beam (with a value of capacitance of 1.8 nF) clamped on a beam holder at one end. A magnet is placed on the other end of the piezoelectric beam. The piezobeam is placed underneath a stepper motor (Phidgets 3303) driven by a bipolar motor control circuit (Phidgets 1067) with a revolving platform mounted on the motor's shaft. The rotating base is divided into two layers in order to achieve voltage peaks synchronization: the bottom layer contains two magnets (5x5x5 mm^3) facing opposite polarity with respect to the tip magnet of the piezoelectric beam. In this way, the piezoelectric beam gets deflected first on one direction (when facing the first magnet), and then on the opposite direction (when facing the second magnet), so that the piezovoltage peaks are properly synchronized with the electromagnetic voltage

peaks. The top layer of the rotating base hosts one magnet that is responsible for the magnetic flux change seen by the coil (with inductance L and resistance r_c of 99 mH and 135 Ω respectively), which is installed inside a plastic case above the rotating base.

3.2. Results

In order to better demonstrate the benefits of the proposed active technique, two different velocities of the rotating base have been tested, corresponding to different frequencies f and, hence, different variation of the open-circuit electromagnetic voltage $V_{EM,oc}$. Figure 10 depicts the experimental waveforms of the hybrid system along with the rectified signals when considering MOSFETs (ZVNL120A, ZVP4424A), Schottky diodes (BAT48) and standard silicon diodes (1N4148) when no load is connected to the circuit. More particularly, figure 10a depicts the experimental waveforms when considering the open circuit electromagnetic voltage $V_{EM,oc}$ of 0.7 V (slightly higher than the typical silicon diode threshold voltage), while figure 10b shows the experimental waveforms when considering the open circuit electromagnetic voltage $V_{EM,oc}$ of 0.4 V (hence, lower than typical silicon diode threshold voltage). Both figures demonstrate the enhancement of the rectified voltage in the hybrid active rectification with respect to the rectification techniques using Schottky diodes and standard diodes. The gap between the different values of rectified voltage is even more evident in figure 11, depicting the rectified voltage on the storing capacitor when using the three different rectification techniques in the transient state. Both cases highlight the notable difference in the voltage values between the proposed hybrid active rectification and the standard rectification methods.

Subsequently, the DC power with a connected load has been measured

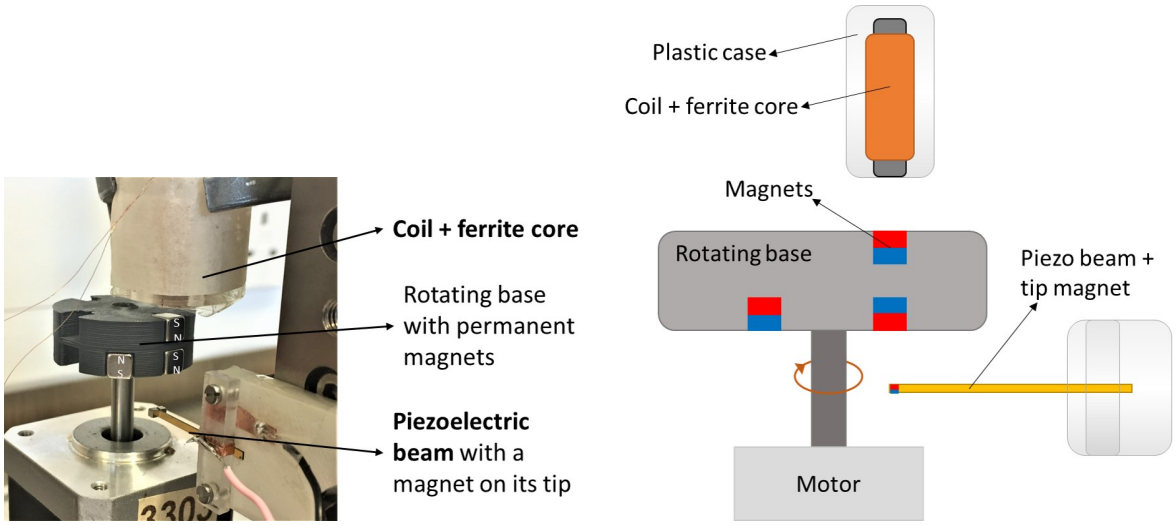

(a) Experimental set-up (b) Experimental set-up schematic

Figure 9: Experimental set-up

considering the three different rectification methods and the two different cases of AC electromagnetic voltage, as shown in figure 12. It is evident from the plot how the rectification in the hybrid cooperative case allows obtaining relatively higher power conversion efficiencies, especially when compared with the non-hybrid techniques. Table 3 compares the maximum output powers P_{max} and the conversion ratio η (following equation 1) between the DC output power $P_{EM,DC}$ and the AC electromagnetic $P_{EM,AC}$ and piezoelectric $P_{PZT,AC}$ powers of the analysed techniques. Moreover, the comparisons among the equivalent conversion ratios η_{DC} with respect to the ideal DC power (as per equation 2) is also given.

Particularly, when considering the case of $V_{EM,oc} = 0.7$ V, it is possible to achieve almost 60% of the AC power (75% of the equivalent DC power when considering ideal diodes), corresponding to a power gain of 27 with respect to value of DC power obtained with standard silicon diodes. When taking into account the case of $V_{EM,oc} = 0.4$ V, the

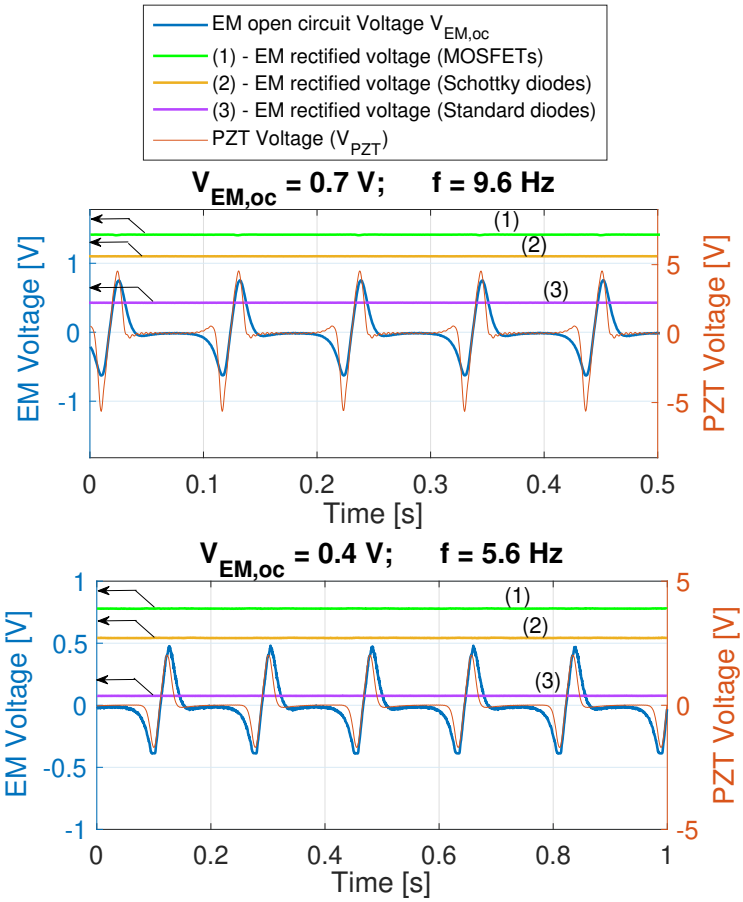

Figure 10: Experimental waveforms (the electromagnetic voltage transducer ($V_{EM,oc}$) and the rectified voltages are given with respect to the left y-axis - specified by the arrows - while the piezoelectric (V_{PZT}) voltage uses the right y-axis) when considering two rotational frequencies (corresponding to two open-circuit voltage magnitudes of the electromagnetic system)

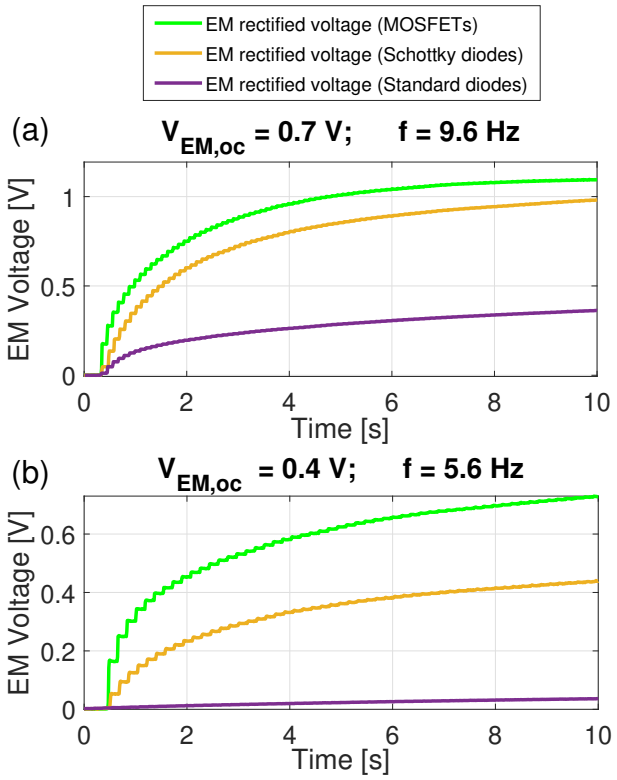

Figure 11: Experimental rectified voltages

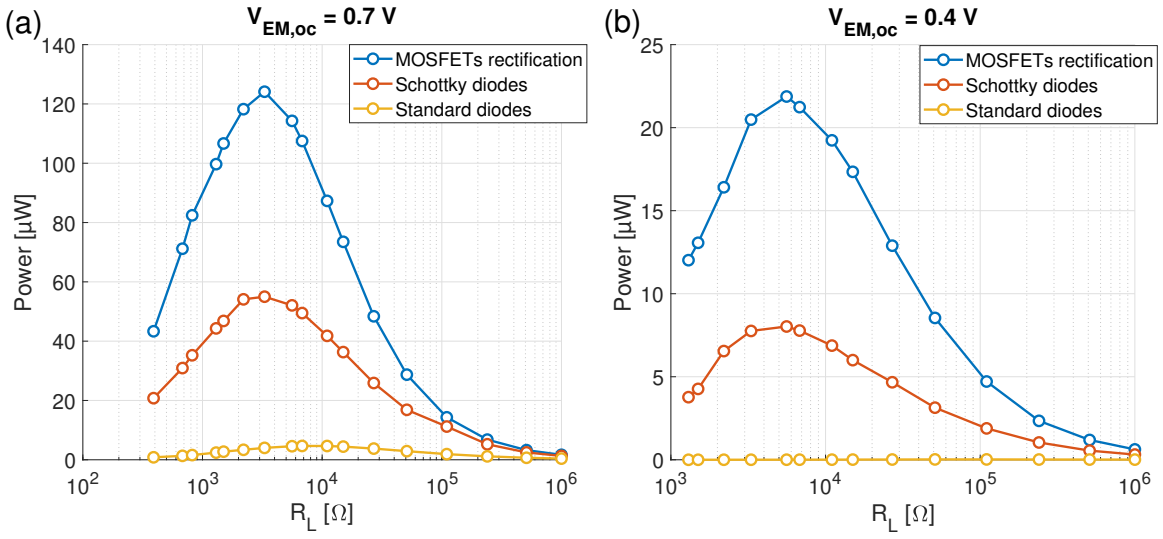

Figure 12: Experimental powers

proposed hybrid technique achieves 30% of the power measured in the AC case (namely 71 μW), while the harvested power measured when considering the standard diodes is almost null, as all the energy is lost within the rectifying stage.

Table 3: Output power level comparisons when considering the case of (a) $V_{EM,oc} = 0.7$ V and (b) $V_{EM,oc} = 0.4$ V

Technique	P_{max}	η	η_{DC}
Hybrid cooperative rectification	a) 125 μW	57 %	75 %
	b) 22 μW	30 %	40 %
Schottky diodes rectification	a) 55 μW	26 %	35 %
	b) 8 μW	11 %	15 %
Standard diodes rectification	a) 4.65 μW	2.25 %	3 %
	b) 0.02 μW	0.03 %	0.04 %

4. Conclusion

The proposed work presented a hybrid cooperative electromagnetic-piezoelectric energy harvesting system addressing in a simple manner the issue of rectification losses in low-power applications. Contrary to typical hybrid systems that aim at using both transducers for actual energy harvesting, the cooperation between the two transducers is achieved by connecting the electromagnetic system to a half-wave voltage doubler circuit employing MOSFETs (in replacement of diodes) which are powered by the piezoelectric element.

Simulations and experimental results have demonstrated the great improvement of the energy conversion efficiency of the electromagnetic transducer with respect to the non-hybrid case employing Schottky diodes and standard diodes, particularly when considering low values of electromagnetic voltage output.

The proposed method thus combines the benefit of a high-efficiency active bridge with the simplicity of passive rectification, overcoming the challenge of cold-starting and power consumption typically required by active rectifiers.

Acknowledgments

The authors gratefully acknowledge the financial support from European Union's Horizon 2020 Research and Innovation Programme under the Marie Skłodowska-Curie Grant Agreement No. 722496.

References

[1] Miorandi D, Sicari S, De Pellegrini F and Chlamtac I 2012 *Ad hoc networks* **10** 1497–1516
[2] Barré A, Deguilhem B, Grolleau S, Gérard M, Suard F and Riu D 2013 *Journal of Power Sources* **241** 680–689
[3] Matiko J, Grabham N, Beeby S and Tudor M 2013 *Measurement Science and Technology* **25** 012002
[4] Shaikh F K and Zeadally S 2016 *Renewable and Sustainable Energy Reviews* **55** 1041–1054

[5] Berney J C 1976 Watch movement driven by a spring and regulated by an electronic circuit uS Patent 3,937,001
[6] Donelan J M, Li Q, Naing V, Hoffer J A, Weber D and Kuo A D 2008 *Science* **319** 807–810
[7] Epstein A H 2003 Millimeter-scale, mems gas turbine engines *ASME Turbo Expo 2003, collocated with the 2003 International Joint Power Generation Conference* (American Society of Mechanical Engineers Digital Collection) pp 669–696
[8] Howey D A, Bansal A and Holmes A S 2011 *Smart Materials and Structures* **20** 085021
[9] Zhang Y, Cao J, Zhu H and Lei Y 2019 *Energy conversion and management* **180** 811–821
[10] Lockhart R, Janphuang P, Briand D and de Rooij N F 2014 A wearable system of micromachined piezoelectric cantilevers coupled to a rotational oscillating mass for on-body energy harvesting *2014 IEEE 27th international conference on micro electro mechanical systems (MEMS)* (IEEE) pp 370–373
[11] Shu Y, Wang W and Chang Y 2018 *Smart Materials and Structures* **27** 125006
[12] Fu H and Yeatman E M 2017 *Energy* **125** 152–161
[13] Pillatsch P, Yeatman E M and Holmes A S 2014 *Sensors and Actuators A: Physical* **206** 178–185
[14] Wu W H, Kuo K C, Lin Y H and Tsai Y C 2018 *Microelectronic Engineering* **191** 16–19
[15] Xue T and Roundy S 2017 *Sensors and Actuators A: Physical* **253** 101–111
[16] 2014 *http://www.farnell.com/datasheets/2167162.pdf*
[17] Leicht J, Maurath D and Manoli Y 2012 Autonomous and self-starting efficient micro energy harvesting interface with adaptive mppt, buffer monitoring, and voltage stabilization *2012 Proceedings of the ESSCIRC (ESSCIRC)* (IEEE) pp 101–104
[18] Szarka G D, Burrow S G, Proynov P P and Stark B H 2013 *IEEE transactions on Power Electronics* **29** 201–212
[19] Maurath D, Becker P F, Spreemann D and Manoli Y 2012 *IEEE Journal of Solid-State Circuits* **47** 1369–1380
[20] Lallart M and Inman D J 2011 Mechanical effect of combined piezoelectric and electromagnetic energy harvesting *Structural Dynamics and Renewable Energy, Volume 1* (Springer) pp 261–272
[21] Zolfaghar Tehrani S, Ranjbar H, Vial P and Premaratne P 2019 *A New Efficient Power Management Interface for Hybrid Electromagnetic-Piezoelectric Energy Harvesting System* pp 537–542 ISBN 978-3-030-14069-4
[22] Xia H, Chen R and Ren L 2015 *Sensors and Actuators A: Physical* **234** 87–98
[23] Liu H, Gao S, Wu J and Li P 2019 Study on the output performance of a nonlinear hybrid piezoelectric-electromagnetic harvester under harmonic excitation *Acoustics* vol 1 (Multidisciplinary Digital Publishing Institute) pp 382–392
[24] Wang P, Pan L, Wang J, Xu M, Dai G, Zou H, Dong K and Wang Z L 2018 *ACS nano* **12** 9433–9440
[25] Rajarathinam M and Ali S 2018 *Energy Conversion and Management* **155** 10–19
[26] Lallart M and Lombardi G 2020 *Energy Conversion and Management* **203** 112135
[27] Collado A and Georgiadis A 2013 *IEEE Transactions on Circuits and Systems I: Regular Papers* **60** 2225–2234
[28] Guo L, Gu X, Chu P, Hemour S and Wu K 2019 *IEEE Transactions on Industrial Electronics*
[29] Virili M, Georgiadis A, Collado A, Niotaki K, Mezzanotte P, Roselli L, Alimenti F and Carvalho N B 2015 *Wireless Power Transfer* **2** 22–31
[30] Gu X, Hemour S, Guo L and Wu K 2018 *IEEE Transactions on Microwave Theory and Techniques* **66** 4178–4190